Regular Article

PHYSICAL CHEMISTRY RESEARCH
Published by the
Iranian Chemical Society
www.physchemres.org
info@physchemres.org

***Phys. Chem. Res.**, Vol. 4, No. 2, 291-301, June 2016.*
DOI: 10.22036/pcr.2016.14114

A Kinetic Study on Adsorption of Congo Red from Aqueous Solution by ZnO-$ZnFe_2O_4$-polypyrrole Magnetic Nanocomposite

A. Karamipour, N. Rasouli*, M. Movahedi and H. Salavati
Department of Chemistry, Payame Noor University, P.O. Box: 19395-3697, Tehran, Iran
(Received 11 December 2015, Accepted 7 April 2016)

In this work, magnetically separable ZnO-$ZnFe_2O_4$-PPy nanocomposite as an efficient adsorbent was synthesized by two steps. At first, zinc oxide (ZnO) and $ZnFe_2O_4$ nanoparticles were synthesized using simple and facile precipitation method. Then, ZnO-$ZnFe_2O_4$ mixed oxide was modified by polypyrrole (PPy). The adsorbent was characterized by X-ray diffraction (XRD), Fourier transform infrared (FT-IR), UV-Vis and scanning electron microscopy (SEM). The synthesized nanocomposite were used as adsorbent to remove Congo red dye from aqueous solution and were compared with pure ZnO and ZnO-PPy adsorbents. The ZnO-$ZnFe_2O_4$-PPy nanocomposite adsorbent showed a superior Congo red removal efficiency than ZnO and ZnO-PPy adsorbents. This efficiency is attributed to the charge of surface obtained in nanocomposite adsorbent. Furthermore, the adsorption kinetics of Congo red onto the nanocomposite followed by the pseudo-second-order kinetic model.

Keywords: ZnO, Polypyrrole, Adsorption, Congo red, Magnetic nanocomposite

INTRODUCTION

Recently, the applications of dyes in versatile industrial processes such as textile, plastic, leather, cosmetics, food, *etc*. are increasing. Since these dye wastes are hazardous, toxic, non-biodegradable and carcinogenic, special attention is given to remove these contaminations from the environment [1]. Many techniques like filtration, coagulation, chemical oxidation, ion exchange, precipitation and adsorption are used for wastewater treatment [2,3]. Nowadays, unique features of "adsorption techniques", such as high efficiency, simplicity and reusability, have made them valuable techniques to remove the dyes from industrial effluents [4,5]. Recently, significant research studies have been conducted on nano-sized adsorbents. The use of nanoparticles as adsorbent to adsorb pollutants is particularly important. This is due to the very small size (high surface to area to volume ratio) and special morphology of nanoparticles to adsorb organic pollutants quickly. Nano-zinc oxide (ZnO) as one of the materials with incredible features such as thermal stability, irradiation resistance, biocompatibility, low cost and flexibility can form different nanostructures [6-9], which has been used in adsorption of dye less than other conventional material. Thus, there is a great interest to use the nano-ZnO with its unique properties in wastewater treatment for dye adsorption. To reduce the surface area and surface energy, nanoscale materials aggregate easily, so many studies have been devoted to stop this phenomenon [10,11]; such as coating the surface of nanoparticles by the polymers [12]. On the other hand, the separation of nanoparticles from solution presents difficulties to a certain extent. Applying the magnetic field would be a highly-efficient separation technique due to the main advantages such as effective control, high speed and simplicity compared to the conventional separation methods [13,14]. In recent years, due to unique properties of spinel $ZnFe_2O_4$, many efforts have been devoted to investigate the $ZnFe_2O_4$-based composites as magnetically separable compounds [15-17]. In this work, Congo red is employed as a model compound

*Corresponding author. E-mail: n.rasouli@pnu.ac.ir

Scheme 1. Molecular structure of Congo red

for common water soluble azo dyes (Scheme 1) widely used in textile industry. This research is aimed at the synthesis of the ZnO-$ZnFe_2O_4$-PPy nanocomposite as adsorbent *via* precipitation method due to its simplicity, low cost and homogeneous dispersion of raw material. The composition and morphology of the synthesized samples are also investigated by FT-IR, XRD, UV-Vis and SEM techniques. Finally, Congo red adsorption capacity of the synthesized samples (ZnO, ZnO-PPy and ZnO-$ZnFe_2O_4$-PPy) are compared with each other. To the best of our knowledge, this work is a novel research for adsorption of Congo red dye on the surface of ZnO-$ZnFe_2O_4$-PPY sample as a magnetically separable adsorbent.

EXPERIMENTAL

All the analytical chemicals ($Fe(NO_3)_3.9H_2O$, $Zn(NO_3)_2.6H_2O$, $Zn(CH_3COO)_2.2H_2O$, Triton X-100, Cetyl trimethyl ammonium bromide, sodium lauryl sulfate, pyrrole, ammonium persulfate, sodium hydroxide and Congo red dye were purchased from Merck and used without further purification.

The structural analysis of the samples was performed by powder X-ray Diffraction (Holland Philips Xpert, X-ray diffractometer with Cu-Kα radiation) and FT-IR analysis using a Fourier transmission infrared spectrometer (JASCO FTIR-4200, Japan) in KBr pellet, in the range of 4000-400 cm^{-1}. The morphology of the samples was characterized by scanning electron microscopy, SEM (VEGA3, TESCAN). The UV-Vis absorption spectra were recorded using a Shimadzu UV-2550 spectrophotometer.

Synthesis of the $ZnFe_2O_4$ Sample

The procedure used for the synthesis of $ZnFe_2O_4$ has been previously reported [18]. In this method, $Fe(NO_3)_3.9H_2O$ (6×10^{-3} mol), $Zn(NO_3)_2.6H_2O$ (3×10^{-3} mol), NaOH (0.040 mol), cetyl trimethyl ammonium bromide (5.48×10^{-4} mol) and 15 ml distilled water were used. The above chemicals were mixed vigorously *via* a magnetic stirrer for 120 min at room temperature, then the obtained solid product was washed several times with deionized water, and dried at room temperature and annealed at 500 ºC for 1 h.

Synthesis of the ZnO Sample

The ZnO sample was prepared *via* precipitation method. In this method, 5.27 g (0.024 mol) of $Zn(CH_3COO)_2.2H_2O$), 2.8 g (0.07 mol) of NaOH, 15 ml distilled water and 0.012 mol of Triton X-100 were used. Then, the obtained mixture was stirred vigorously on magnetic stirrer for 120 min at room temperature. Finally, the obtained solid washed several times with deionized water, dried at room temperature and annealed at 500 ºC for 1 h.

Synthesis of the ZnO-$ZnFe_2O_4$-PPy Composite

The procedure used for the synthesis of the $ZnFe_2O_4$-ZnO has been reported, previously [19]. In this procedure, 0.15 g (2×10^{-4} mol) $ZnFe_2O_4$ and 0.05 g (6×10^{-4} mol) ZnO were mixed with a 40 ml aqueous solution containing of 1.4×10^{-5} mol sodium lauryl sulfate sonicated for 30 min and stirrered mechanically for 3 h. After adding of 25.8 ml pyrrole monomer, the solution was continuously stirred for another 1 h. Then, 11.2 ml of the 0.1 M ammonium

persulfate solution was added drop wise into the above solution. The polymerization process was conducted while stirring for 4 h at room temperature. The product was magnetically separated, washed with deionized water, ethanol and dried in oven at 80 ºC.

Adsorption Experiments

The adsorption behavior of the ZnO-$ZnFe_2O_4$-PPy sample was evaluated by decolorization of Congo red dye solution. The adsorption experiments were performed under the same conditions (50 mg l^{-1} initial concentration of Congo red dye solution, 0.5 g l^{-1} adsorbent dosage and t = 25 °C). The samples were taken during regular intervals and the adsorbent was removed by applying an external magnetic field. Then, the degree of adsorption (X), as a function of time is given by $X = (C_\circ - C)/C_\circ$ where $C_\circ$ and C are the initial concentration and the concentration of dye at time t. The disappearance of peak at $\lambda = 498$ nm was chosen for monitoring of Congo red adsorption. The same experiments were also performed for ZnO and ZnO-PPy

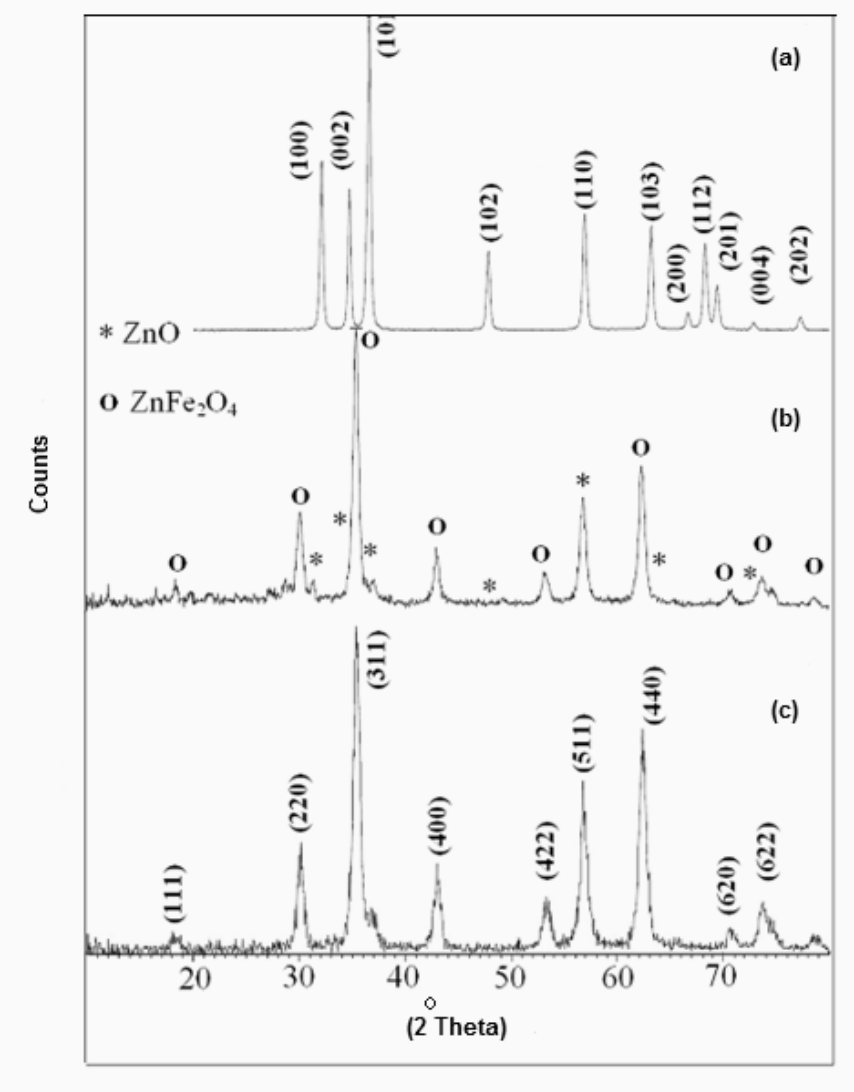

Fig. 1. The XRD patterns of (a) ZnO, (b) ZnO-$ZnFe_2O_4$-PPy and (c) $ZnFe_2O_4$.

samples to compare the results.

RESULTS AND DISCUSSION

Characterization

Figures 1a-c shows the XRD patterns of ZnO, ZnO-$ZnFe_2O_4$-PPy and $ZnFe_2O_4$, respectively. The results confirm the presence of cubic phase $ZnFe_2O_4$ (JCPDS No. 82-1049), and well matching of the distinctive peaks at 29.92°, 35.27°, 42.85°, 53.11°, 56.63° and 62.21° with the (220), (311), (400), (422), (511) and (440) crystal planes of $ZnFe_2O_4$. Other crystal phases corresponding to the peaks at 31.8°, 34.4°, 36.3°, 47.5°, 68.0° and 69.1° indicate the presence of ZnO (JCPDS No. 36-1451). It is worthy of notice that the characteristic diffraction peak of ZnO in the ZnO-$ZnFe_2O_4$-PPy composite was weak, which could be attributed to the low amount of ZnO used in the synthesis of ZnO-$ZnFe_2O_4$-PPy. In case of the ZnO-$ZnFe_2O_4$-PPy composite, the peaks corresponding to the polypyrrole cannot be detected indicatig that the polypyrrole is amorphous. The chemical structure of the ZnO-$ZnFe_2O_4$-PPy composite was confirmed by FT-IR analysis. Figures

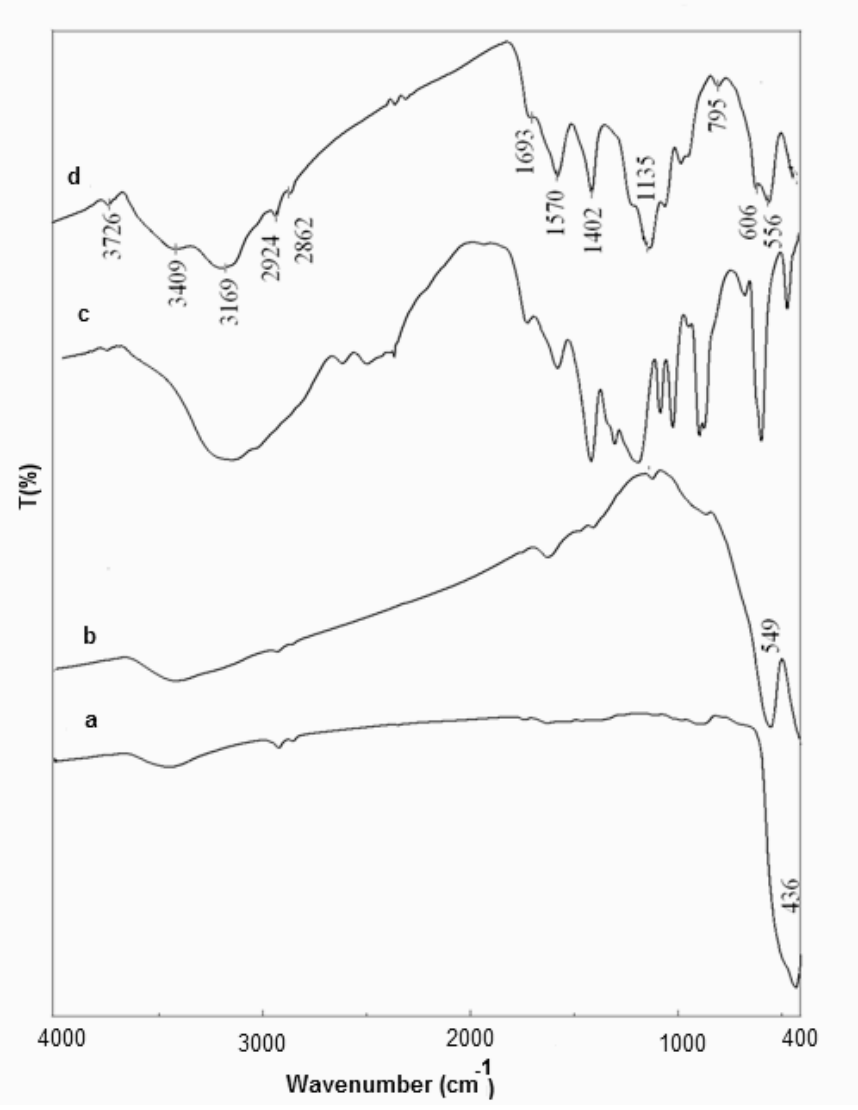

Fig. 2. The FT-IR spectra of (a) ZnO, (b) $ZnFe_2O_4$, (c) PPy and (d) ZnO-$ZnFe_2O_4$-PPy.

2a-d shows the FT-IR spectra of ZnO, $ZnFe_2O_4$, ZnO-$ZnFe_2O_4$-PPy and PPy in the region of 400-4000 cm^{-1}. In Fig. 2a, the band at 436 cm^{-1} was ascribed to the Zn-O stretching vibrations [20]. In Fig. 2b, for $ZnFe_2O_4$, two characteristic peaks observed at around 410 and 549 cm^{-1} correspond to intrinsic stretching vibrations of the metal at the octahedral and tetrahedral sites, respectively [21,22]. In Fig. 2c, the stretching vibration at 3115 cm^{-1} can be attributed to the N-H stretching vibrations of the polypyrrole. For pure PPy, all the characteristic peaks are observed at 794 cm^{-1} (=C-H wagging) [23], 926 cm^{-1} (C-C out of phase), 1048 cm^{-1} (=C-H in plane vibration), 1292 cm^{-1} (C-C bond), 1478 cm^{-1} (vibration of the pyrrole ring), 1558 cm^{-1} (C=C bond) and 1705 cm^{-1} (C=N bond). The peaks observed in FT-IR of PPy coincide well with the ones available in literature [24], indicating the presence of polypyrrole. In ZnO-$ZnFe_2O_4$-PPy nanocomposite, peak at 3409 cm^{-1} is indicative of -OH stretching vibrations of the adsorbed water molecules [25]. The FT-IR spectrum of ZnO-$ZnFe_2O_4$-PPy composite (Fig. 2d) shows some shift as well as changes in the intensity of peaks compared to PPy and the results show that polypyrrole has been successfully used in the composite. As a result of delocalized electrons on the polypyrrole ring, the oxidation of poylpyrrole can be avoided [26,24]. The band at 441 cm^{-1} confirmed the presence of ZnO in the ZnO-$ZnFe_2O_4$-PPy composite [27]. The results have shown that the polymerization is carried out successfully. Figure 3 shows the UV-Vis diffuse relectance spectra of the ZnO, ZnO-PPy and ZnO-$ZnFe_2O_4$-PPy samples. The ZnO nanoparticles has a strong absorption in the ultraviolet region and in the wavelength between 250 and 400 nm (λ_{max}= 359 nm), similar to that reported by Wang *et al*. [28]. The ZnO-PPy sample show absorption at wavelengths of 282 and 351 nm (Fig. 3b). The peak at about 282 nm is related to the presence of the PPy. The absorption bands in the sample containing $ZnFe_2O_4$ is in the range of 460-670 nm which can use as photocatalyst in the visible region [29] (Fig. 3c). The morphology of ZnO, ZnO-PPy and ZnO-$ZnFe_2O_4$-PPy can be relized in the SEM images (Figs. 4a-4c). The particle size of ZnO is approximately 30-100 nm according to SEM (Fig. 4a). However, SEM image of the ZnO-PPy sample is different from ZnO sample [18]. Based on the results of XRD, FT-IR, SEM and UV-Vis confirmed the synthesis of the ZnO-$ZnFe_2O_4$-PPy composite.

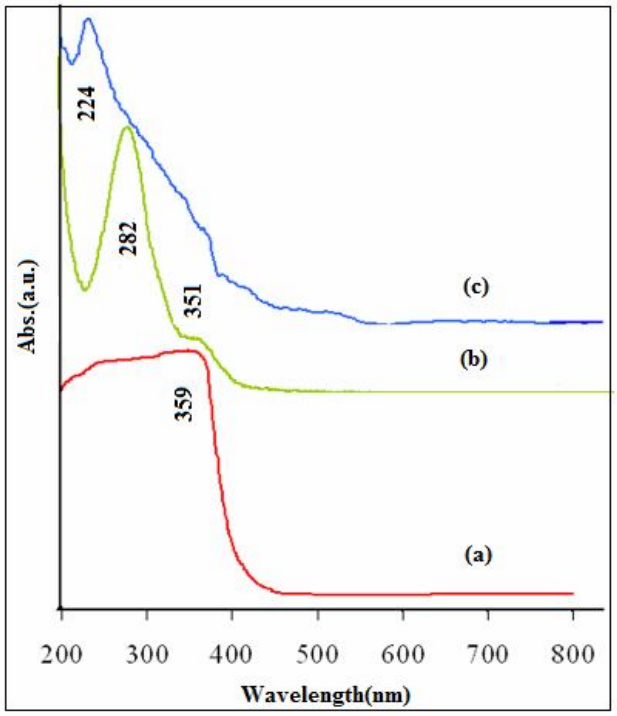

Fig. 3. UV-Vis absorption spectra of (a) ZnO (b), ZnO-PPy, (c) ZnO-$ZnFe_2O_4$-PPy.

The Adsorption Behavior of Congo Red on ZnO-$ZnFe_2O_4$-PPy

In order to investigate the behavior of the ZnO-$ZnFe_2O_4$-PPy composite, dark adsorption experiments were carried out. The amount of adsorbed dye per gram of adsorbent (mg g^{-1}) at time t (min) was calculated using the following equation [30]:

$$q_t = \frac{(C_0 - C_t)V}{m} \quad (1)$$

where q_t (mg g^{-1}) is the amount of adsorbed Congo red per gram of adsorbent at time t (min), C_0 is the initial concentration of Congo red solution (mg l^{-1}), C_t is the concentration of Congo red solution (mg l^{-1}) at time t (min), V is the volume of the solution (l) and m is the mass of the adsorbent (g). Figure 5 shows Congo red adsorption

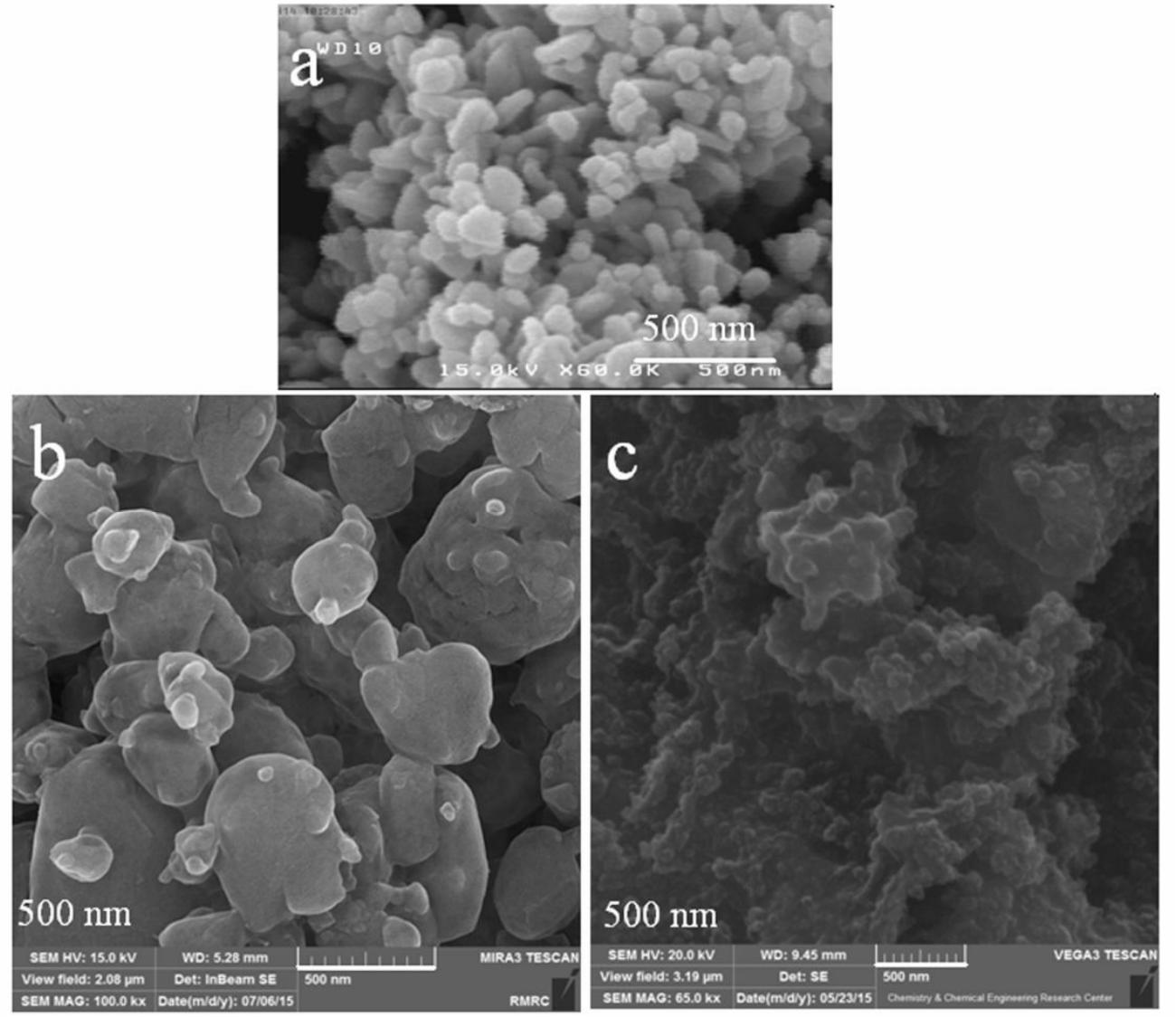

Fig. 4. The SEM images of (a) ZnO, (b) ZnO-PPy and (c) ZnO-$ZnFe_2O_4$-PPy.

percentage on the surface of synthesized samples versus time. The results showed that 25, 40 and 78 percent of Congo red dye is absorbed on the surface of the ZnO, ZnO-PPy and ZnO-$ZnFe_2O_4$-PPy, respectively. Figure 6 shows the adsorption capacity of the synthesized samples versus time. As shown in Fig. 6, adsorption capacity of the synthesized samples are changed accordingly:

ZnO-$ZnFe_2O_4$-PPy (74 mg g^{-1}) > ZnO-PPy (38 mg g^{-1}) > ZnO (24 mg g^{-1}).

Effect of pH

The initial pH of dye solution plays an important role in adsorption process [31]. The effect of pH is studied between 4 and 9 because at strong acidic medium, the color of Congo red solution changes from red to dark blue and the original red color is different above pH 10. As shown in Fig. 7, the maximum of removal efficiency on the surface of ZnO-$ZnFe_2O_4$-PPy sample is achieved in the acidic medium (98%) and reduced at the basic medium (47%). In the acidic

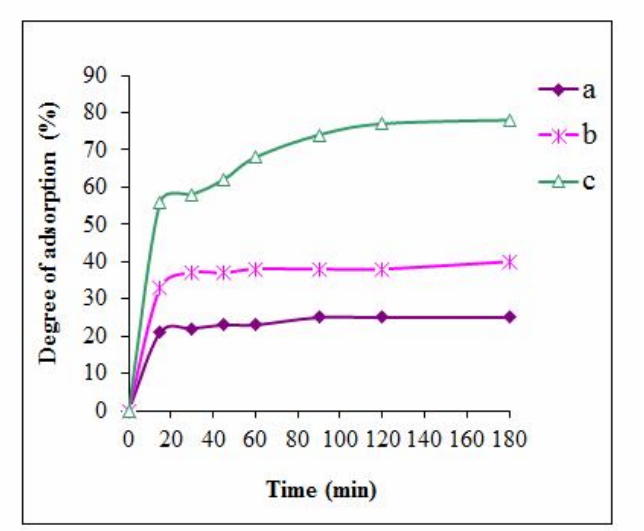

Fig. 5. Plots of the adsorption percentage for Congo red dye on: (a) ZnO, (b) ZnO-PPy and (c) ZnO-$ZnFe_2O_4$-PPy.

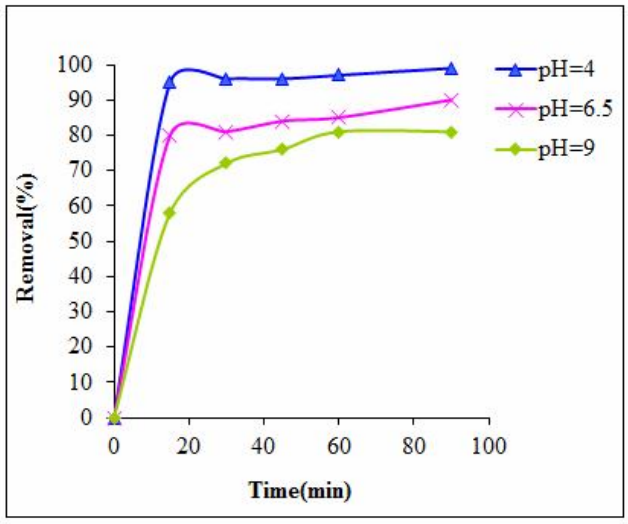

Fig. 7. Effect of pH on adsorption of Congo red on the ZnO-$ZnFe_2O_4$-PPy sample.

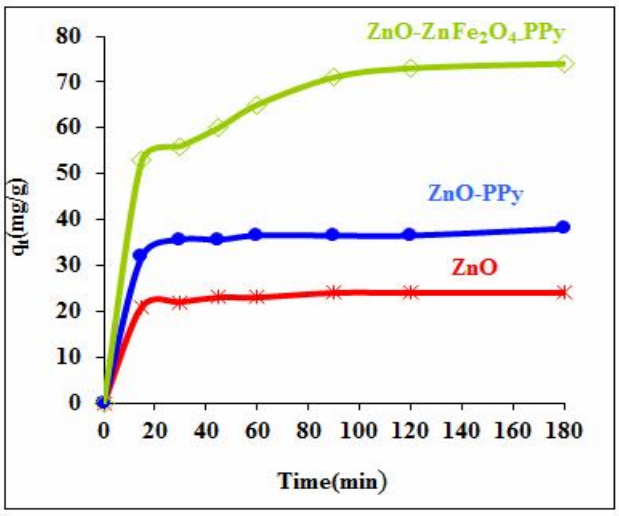

Fig. 6. Adsorption capacity of (a) ZnO, (b) ZnO-PPy and (c) ZnO-$ZnFe_2O_4$-PPy.

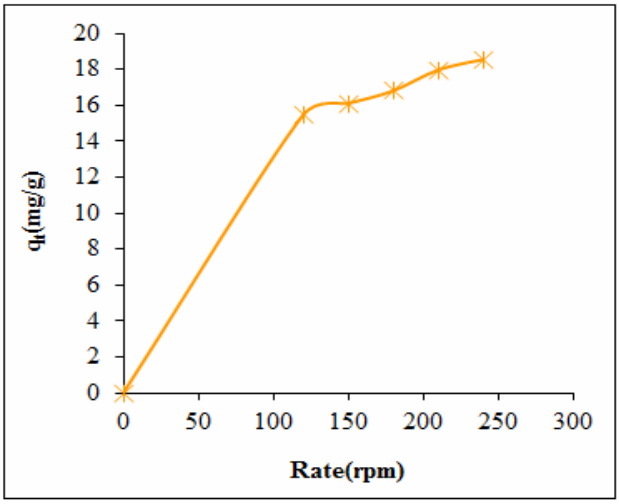

Fig. 8. Effect of the agitation speed on adsorption capacity of Congo red on the ZnO-$ZnFe_2O_4$-PPy sample.

medium, the solution of Congo red will be in cationic form [32] and the adsorption of cation would be favorable at pH > pH_{zp} [33]. When transferring from acidic to basic medium, due to the electrostatic repulsion, the removal efficiency is reduced. In the basic medium (pH = 10-12) there would be a competion between anionic dye and OH^- in sluosion [34].

Effect of Agitation Speed

The effect of agitation speed on Congo red dye removal on the surface of ZnO-$ZnFe_2O_4$-PPy sample is shown in Fig. 8, as agitation speed increases from 100 to 250 rpm. At lower speed, the lower adsorption capacity is due to the poor interaction between adsorbate and adsorbent. As the speed reaches to 250 rpm, an increase in the adsorption

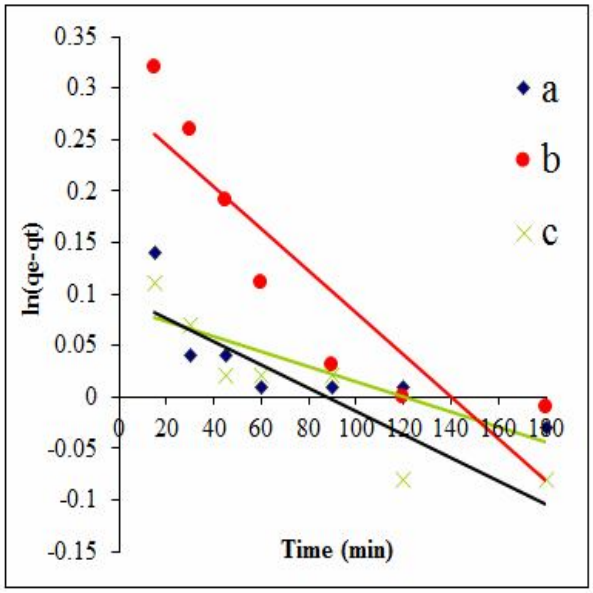

Fig. 9. Plot $\ln(q_e-q_t)$ *vs.* time (pseudo-first-order model) for the (a) ZnO-PPy, (b) ZnO-$ZnFe_2O_4$-PPy and (c) ZnO samples.

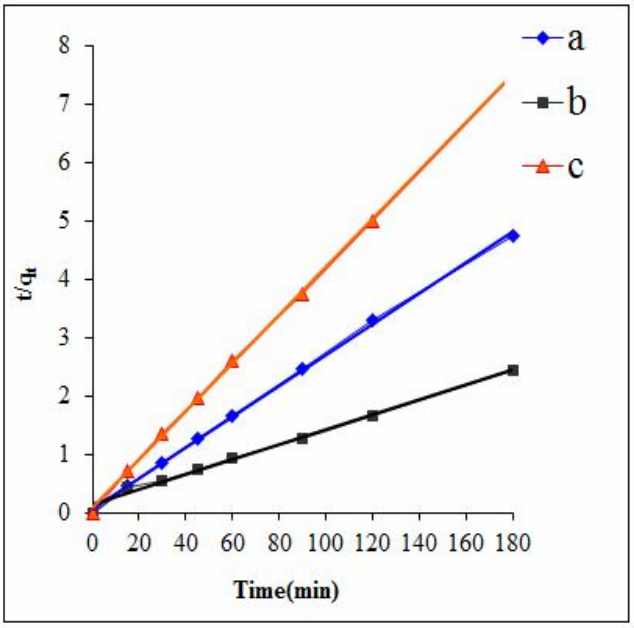

Fig. 10. Plot of t/q_t *vs.* time (pseudo-second-order model) for the (a) ZnO-PPy, (b) ZnO-$ZnFe_2O_4$-PPy and (c) ZnO samples.

capacity is observed, while adsorption capacity does not show a significant variation at rates above 250 rpm. Thus, 250 rpm is considered as the optimum agitation speed for the removal of Congo red dye.

Adsorption Kinetics

The study of adsorption kinetics provided valuable insight into the reaction pathways and the mechanism of the reaction [35]. Several kinetic models have been used to study the kinetics of the adsorption process: the pseudo-first-order and pseudo-second-order kinetic models.

Pseudo-first-order Kinetic Model

The kinetics of adsorption can be described using several models. A simple kinetic model is the pseudo-first-order equation [36]:

$$\frac{dq_t}{dt} = k_1 (q_e - q_t) \quad (2)$$

After definite integration by applying the initial conditions, $q_t = 0$ at $t = 0$ and $q_t = q_t$ at $t = t$, Eq. (2) becomes:

$$\ln(q_e - q_t) = \ln q_e - k_1 t \quad (3)$$

where q_e and q_t are the amounts of adsorbate adsorbed (mg g^{-1}) at equilibrium and at any instant of time t (min), respectively, and k_1 is the rate constant for pseudo-first-order adsorption (min^{-1}). The adsorption rate constant k_1 and equilibrium adsorption capacity $q_{e,cal}$, calculated from the slopes and intercepts of plots of $\log(q_e - q_t)$ *vs.* t (Fig. 9) along with correlation coefficients R^2 are listed in Table 1. As shown in Table.1, the experimental $q_{e,exp}$ values are not in agreement with the calculated ones obtained from the linear plots. The results show that adsorption of Congo red on synthesized samples do not follow the first order kinetics model.

Pseudo-second-order Equation Kinetic Model

The pseudo-second-order kinetic model based on equilibrium adsorption can be represented by the Eq. (4) [37]:

$$\frac{t}{q_t} = \frac{1}{k_2 q_e^2} + \frac{1}{q_e t} \quad (4)$$

Table 1. Kinetic Adsorption Parameters Obtained Using Pseudo-first-order and Pseudo-second-order Methods

Sample	q_e^{exp} (mg g^{-1})	Pseudo-first-order			Pseudo-second-order		
		k_1 (min^{-1})	q_{e1} (mg g^{-1})	R^2	k_2 (g mg^{-1} min^{-1})	q_{e2} (mg g^{-1})	R^2
ZnO-PPy	37	0.0007	1.09	0.6216	0.012	38	0.9993
ZnO-$ZnFe_2O_4$-PPy	73	0.0020	1.33	0.8037	0.0012	78	0.9922
ZnO	24	0.0011	2.67	0.8433	0.5208	24	0.9997

where k_2 is the equilibrium rate constant of pseudo-second-order adsorption (g mg^{-1} min). The straight line plots of t/q_t versus time as shown in Fig. 10 have been used to obtain the rate parameters. The values for q_e and k_2 along with the correlation coefficient (R^2) values are presented in Table 1. It can be found from Table 1 that the calculated q_e values agree well with those of experimentally obtained q_e for the pseudo-seond-order model. Furthermore, the correlation coefficient values obtained by fitting the experimental data to Eq. (4) were close to 1.0. The calculated q_e values also agree very well with the experimental data in the case of pseudo-second-order kinetics suggesting that the rate-limiting step may be chemical sorption or chemisorption involving valency forces through sharing or exchanging of electrons between the samples and dye ions [38].

CONCLUSIONS

In our study, ZnO-$ZnFe_2O_4$-PPy nanocomposite was prepared by chemical precipitation method as a simple and and effective method and used as adsorbent for Congo red removal from the aqueous solution. The results show that three-component composite (ZnO-$ZnFe_2O_4$-PPy) as an adsorbent is more efficient compared to ZnO and ZnO-PPy species for color removal. Therefore, it can be concluded that the low cost ZnO-$ZnFe_2O_4$-PPy nanocomposite is an efficient adsorbent for removal of azo dyes from industrial wastewater.

ACKNOWLEDGEMENTS

We are grateful to the Research Council of Payame Noor University for their financial supports.

REFERENCES

[1] Bhatangar, A.; Jain, A. K., A comparative adsorption study with different industrial wastes as adsorbents for the removal of cationic dyes from water. *J. Colloid Interface Sci.*, **2005**, *281*, 49-55, DOI: 10.1016/j.jcis.2004.08.076.

[2] Ong, S. T.; Keng, P. S.; Lee, W. N.; Ha, S. T.; Hung, Y. T., Dye waste treatment. *Water*, **2011**, *3*, 157-176, DOI: 10.3390/w3010157.

[3] Jiuhui, Q., Research progress of novel adsorption processes in water purification: a review. *J. Environ. Sci.*, **2008**, *20*, 1-13, DOI: 10.1016/S1001-0742(08)60001-7.

[4] Gupta, V. K., Application of low-cost adsorbents for dye removal-A review. *J. Environ. Manage*. **2009**, *90*, 2313-2342, DOI: org/10.1016/ j.jenvman.2008.11.017.

[5] Jalil, A. A.; Triwahyonob, S.; Hazirah-Adama, S.; Diana-Rahima, N.; Aziza, M. A. A.; Hairmoc, N. H.; Razalia, N. A. M.; Abidina, M. A. Z.; Mohamadiaha, M. K. A., Adsorption of methyl orange from aqueous solution onto calcined Lapindo volcanic mud. *J.*

Hazard. Mater., **2010**, *181*, 755-762, DOI: 10.1016/j.jhazmat.2010.05.078.

[6] Wang, Z. L., Zinc oxide nanostructures:growth, properties and applications. *J. Phys. Condens. Matter.*, **2004**, *16*, 829-858, DOI: 10.1088/0953-8984/16/25/R01.

[7] Xu, F.; Lu, Y.; Xie, Y.; Liu, Y., Controllable morphology evolution of electrodeposited ZnO nano/micro-scale structures in aqueous solution. *Mater. Design*, **2009**, *30*, 1704-1711, DOI: 10.1016/j.matdes.2008.07.024.

[8] Cho, S.; Jung, S. H.; Lee, K. H., Morphology-controlled growth of ZnO nanostructures using microwave irradiation: from basic to complex structures. *J. Phys. Chem. C*, **2008**, *112*, 12769-12776, DOI: 10.1021/jp803783s.

[9] Qu, X.; Jia, D., Controlled growth and optical properties of Al^{3+} doped ZnO nanodisks and nanorod clusters. *Mater. Lett.*, **2009**, *63*, 412-414, DOI: 10.1016/j.matlet.2008.10.069.

[10] Nabiyounil, G.; Barati, A.; Saadat, M., Surface adsorption of polyethylene glycol and polyvinyl alcohol with variable molecular weights on zinc. *Iran. J. Chem. Eng.*, **2011**, *8*, 20-30.

[11] Tajizadehgan, H.; Jafari, M.; Rashidzadeh, M.; Teluri, A., A high activity adsorbent of ZnO-Al_2O_3 nanocomposite particles: Synthesis, characterization and dye removal efficiency. *Appl. Surf. Sci.*, **2013**, *276*, 317- 322, DOI: 10.1016/ j.apsusc.2013.03.089.

[12] Girigoswami, K.; Visnanathan, M.; Murugesan, R.; Girigoswami, A., Studies on polymer-coated zinc oxide nanoparticles: UV-blocking efficacy and *in vivo* toxicity. *Mater. Sci. Eng.: C*, **2015**, *56*, 501-510, DOI: 10.1016/j.msec.2015.07.017.

[13] Qu, S.; Huang, F.; Yu, S.; Chen, G.; Kong, J., Magnetic removal of dyes from aqueous solution using multi-walled carbon nanotubes filled with Fe_2O_3 particles. *J. Hazard. Mater.*, **2008**, *160*, 643-647, DOI: 10.1016/j.jhazmat.2008.03.037.

[14] Yang, N.; Zhu, S.; Zhang, D.; Xu, S., Synthesis and properties of magnetic Fe_3O_4-activated carbon nanocomposite particles for dye removal. *Mater. Lett.*, **2008**, *62*, 645-647, DOI: 10.1016/ j.matlet.2007.06.049.

[15] Veith, M.; Hass, M.; Huch, V., Single source precursor approach for the sol-gel synthesis of nanocrystalline $ZnFe_2O_4$ and zinc-iron oxide composites. *Chem. Mater.*, **2005**, *17*, 95-101, DOI: 10.1021/cm0401802.

[16] Li, X. Y.; Hou, Y.; Zhao, Q. D.; Teng, W.; Hu, X. J.; Chen, G. H., Capability of novel $ZnFe_2O_4$ nanotube arrays for visible-light induced degradation of 4-chlorophenol. *Chemosphere*, **2011**, *82*, 581-586, DOI: 10.1016/j.chemosphere.2010.09.068.

[17] Yuan, Z. H.; Zhang, L. D., Synthesis, characterization and photocatalyticactivity of $ZnFe_2O_4/TiO_2$ nanocomposite. *J. Mater. Chem.*, **2001**, *11*, 1265-1268, DOI: 10.1039/B006994I.

[18] Liu, R.; Li, D.; Wang, C.; Li, N.; Li, Q.; Lu, X.; Spendelow, J. S.; Wu, G., Core-shell structured hollow SnO_2-polypyrrole nanocomposite anodes with enhanced cyclic performance for lithium-ion batteries. *Nano Energy*, **2014**, *6*, 73-81, DOI: 10.1016/j.nanoen.2014.03.010.

[19] Hamedani, N. F.; Farzaneh, F., Synthesis of ZnO nanocrystals with hexagonal (wurtzite) structure in water using microwave irradiation. *J. Sci. Islam. Repub. Iran.*, **2006**, *17(3)*, 231-234.

[20] Koseoglu, Y.; Baylkal, A.; Toprak, M. S.; Gozuak, F.; Basaran, A. C.; Aktas, B., Synthesis and characterization of $ZnFe_2O_4$ magnetic nanoparticles *via* a PEG-assisted route. *J. Alloys Compd.*, **2008**, *462* , 209-213, DOI: 10.1016/j.jallcom.2007.07.121.

[21] Pascuta, P.; Borodi, G.; Bosca, M.; Pop, L.; Rada, S.; Culea, E., Structural and physical characteristics of $xGd_2O_3(100\text{-}x)[Bi_2O_3\ B_2O_3]$ glasses. *J. Phys. Conf. Ser.*, **2009**, *182*, 1-5, DOI: 10.1088/1742-6596/182/ 1/012062 .

[22] Eisazadeh, H., Studying the characteristics of polypyrrole and its composites. *World J. Chem.*, **2007**, *2*, 67-74.

[23] Lei, J.; Liang, W.; Martin, C. R., Infrared investigations of pristine, doped and partially doped polypyrrole. *Synth. Met.*, **1992**, *48*, 301-312, DOI: 10.1016/0379-6779(92)90233-9.

[24] Sharifi, I.; Shokrollahi, H., Nanostructural, magnetic and mossbauer studies of nanosized $Co_{1-x}Zn_xFe_2O_4$

synthesized by co-precipitation. *J. Mag. Magn. Mater.*, **2012**, *324*, 2397-2403, DOI: 10.1016/ j.jmmm.2012.03.008.

[25] Shiigi, H.; Kishimoto, M.; Yakabe, H.; Deore, B.; Nagaoka, T., Highly selective molecularly imprinted over oxidized polypyrrole colloids: one-step preparation technique. *Anal. Sci.*, **2002**, *18*, 41-44, DOI: 10.2116/analsci.18.41.

[26] Kumar, A.; Prasad, B.; Mishra, I. M., Adsorptive removal of acrylonitrile by commercial grade activated carbon: Kinetics, equilibrium and thermodynamics. *J. Hazard. Mater.*, **2008**, *152*, 589-600, DOI: 10.1016/j.jhazmat.2007.07.048.

[27] Wang, Z.; Xiao, P.; Qiao, L.; Meng. X.; Zhang. Y.; Li, X.; Yang, F., Polypyrrole sensitized ZnO nanorod arrays for efficient photo-electrochemical splitting of water. *Phys. B Condens Matter.*, **2013**, *419*, 51-56, DOI: 10.1016/j.physb.2013.03.021.

[28] Sua, M. H.; Hea, C.; Sharmab, V. K.; Asi, M. A.; Xia, D.; Li, X. Z.; Deng, H. Q.; Xiong, Y., Mesoporous zinc ferrite: synthesis, characterization, and photocatalytic activity with H_2O_2/visible light. *J. Hazard. Mater.*, **2012**, *212*, 95-103, DOI: 10.1016/ j.jhazmat.2011.10.006.

[29] Ren, Y.; Li, N.; Feng, J.; Luan, T.; Wen, Q.; Li, Z.; Zhang, M., Adsorption of Pb(II) and Cu(II) from aqueous solution on magnetic porous ferrospinel $MnFe_2O_4$. *J. Colloid Interface Sci.*, **2012**, *367*, 415-421, DOI: 10.1016/j.jcis.2011.10.022.

[30] Lata, H.; Garg, V.; Gupta, R., Adsorptive removal of a basic dye by chemically activated parthenium biomass: Equilibrium and Kinetic modeling. *Desalination*, **2008**, *219*, 250-261, DOI: 10.1016/ j.desal.2007.05.018.

[31] Hameed, B. H., Evaluation of papaya seeds as a novel non-conventional low cost adsorbent for removal of methylene blue. *J. Hazard. Mater.*, **2009**, *162*, 939-944, DOI: 10.1016/j.jhazmat.2008.05.120.

[32] Ravirta, J.; Butista, I.; Ferro, M. A.; Castilla, M., Activated carbon surface modification by absorption of bacteria and their effect on aqueous lead absorption. *J. Chem. Technol. Biot.*, **2001**, *76*, 1209-1215, DOI: 10.1002/jctb.506.

[33] Vimonses, V.; Lei, S.; Jina, B., Kinetic study and equilibrium isotherm analysis of Congo Red adsorption by clay materials. *Chem. Eng. J.*, **2009**, *148*, 354-364, DOI: 10.1016/j.cej.2008.09.009.

[34] Baral, S. S.; Das, N.; Chaudhury, G. R.; Das, S. N., A preliminary study on the adsorptive removal of Cr(VI) using seaweed, Hydrilla verticillata. *J. Hazard. Mater*, **2009**, *171*, 358-369, DOI: 10.1016/ j.jhazmat.2009.06.011.

[35] Alpat, S. K.; Ozbayrak, O.; Alpat, S.; Akcay, H., The adsorption kinetics and removal of cationic dye, toluidine blue O, from aqueous solution with Turkish zeolite. *J. Hazard. Mater.*, **2008**, *151*, 213-220, DOI: 10.1016/j.jhazmat.2007.05.071.

[36] Sing, K. K.; Rastogi, R.; Hasan, S. H., Removal of Cr(VI) from wastewater using rice bran. *J. Colloid Interface Sci.*, **2005**, *290*, 61-68, DOI: /10.1016/ j.jcis.2005.04.011.

[37] Ho, Y. S.; Mckay, G., Pseudo-second order model for sorption processes. *Process Biochem.*, **1999**, *34*, 451-465, DOI: 10.1016/S0032-9592(98)00112-5.